




## Article

# Kalithallite, $K_3Tl^{3+}Cl_6 \cdot 2H_2O$ , a new mineral with trivalent thallium from the Tolbachik volcano, Kamchatka, Russia

Igor V. Pekov<sup>1\*</sup>, Maria G. Krzhizhanovskaya<sup>2</sup> , Vasily O. Yapaskurt<sup>1</sup>, Dmitry I. Belakovskiy<sup>3</sup>, Evgeny G. Sidorov<sup>4,†</sup> and Pavel S. Zhegunov<sup>4</sup>

<sup>1</sup>Faculty of Geology, Moscow State University, Leninskie Gory, 119991 Moscow, Russia; <sup>2</sup>Department of Crystallography, St Petersburg State University, University Embankment 7/9, 199034 St Petersburg, Russia; <sup>3</sup>Fersman Mineralogical Museum of Russian Academy of Sciences, Leninsky Prospekt 18-2, 119071 Moscow, Russia; and <sup>4</sup>Institute of Volcanology and Seismology, Far Eastern Branch of the Russian Academy of Sciences, Piip Bulevard 9, 683006 Petropavlovsk-Kamchatsky, Russia

### Abstract

A new mineral kalithallite,  $K_3Tl^{3+}Cl_6 \cdot 2H_2O$ , was found in an active fumarole belonging to the Northern fumarole field at the First scoria cone of the Northern Breakthrough of the Great Tolbachik Fissure Eruption, Tolbachik volcano, Kamchatka, Russia. Kalithallite is a product of the relatively low-temperature (70–150°C) interactions involving high-temperature sublimate minerals, volcanic gas and atmospheric water vapour. The associated minerals are cryobrostryxite,  $KZnCl_3 \cdot 2H_2O$ , halite, sylvite, opal and gypsum. Kalithallite forms lamellar to tabular crystals up to  $5 \times 30 \times 40 \mu m$  combined in open-work aggregates up to 1 mm across. It is transparent, colourless in individuals and white to pale cream coloured or pale beige in aggregates, with vitreous lustre.  $D_{calc} = 3.01 \text{ g cm}^{-3}$ . Kalithallite is optically uniaxial (–),  $\epsilon = 1.656(3)$  and  $\omega = 1.662(3)$ . The chemical composition (wt.%, electron-microprobe data,  $H_2O$  calculated by stoichiometry) is: K 17.72, Zn 0.85, Tl 38.76, Cl 35.91,  $H_2O_{calc}$  5.99, total 99.23. The empirical formula calculated on the basis of  $K+Zn+Tl+Cl = 10$  apfu is  $K_{2.72}Zn_{0.06}Tl_{1.14}Cl_{6.08} \cdot 2H_2O$ . Kalithallite is tetragonal,  $I4/mmm$ ,  $a = 15.9333(5)$ ,  $c = 18.1088(7) \text{ \AA}$ ,  $V = 4595.2(4) \text{ \AA}^3$  and  $Z = 14$ . The strongest reflections of the powder X-ray diffraction (XRD) pattern [ $d, \text{ \AA}(I)(hkl)$ ] are: 5.98(100)(202); 5.64(36)(220); 3.984(20)(400); 3.528(30)(224); 3.315(22)(422); 2.890(15)(334); and 2.817(24)(206, 440). Kalithallite is isotypical to synthetic  $K_3Tl^{3+}Cl_6 \cdot 2H_2O$ . The crystal structure was refined from the powder XRD data using the Rietveld method,  $R_{Bragg} = 0.55\%$ ,  $R_p = 0.56\%$ , and  $R_{wp} = 0.75\%$ . The structure contains  $Tl^{3+}Cl_6$  octahedra and K-centred polyhedra of three types:  $KCl_8$ ,  $KCl_8(H_2O)$  and  $KCl_7(H_2O)_2$ . The mineral is named as a *kalium–thallium* ordered compound.

**Keywords:** kalithallite, new mineral, trivalent thallium, potassium thallium chloride, crystal structure, fumarole, Tolbachik volcano, Kamchatka

(Received 18 September 2022; accepted 4 November 2022; Accepted Manuscript published online: 21 November 2022; Associate Editor: Owen Peter Missen)

### Introduction

Thallium is considered a rare chemical element in terms of its abundance in the Earth's crust: its average content in the upper continental crust is  $0.9 \mu g g^{-1}$  (Rudnick and Gao, 2003). Despite minor amounts in Nature, thallium demonstrates a diverse mineralogy that is caused by its specific crystal chemical features that allow this element to concentrate in the crystal structures of many minerals, especially sulfosalts (Zemann, 1993). Eighty-two valid minerals with species-defining Tl are currently approved by the International Mineralogical Association (IMA), including 66 chalcogenides, mainly sulfosalts with As or/and Sb (57 species). Seven thallium minerals are oxysalts (five of which are sulfates), two species belong to oxides, six to halides (five chlorides and one iodide), and one to intermetallic compounds.

Thallium minerals of different chemical classes have different genesis: chalcogenides and the intermetallic compound form in hydrothermal, typically low-temperature ore deposits with sulfide or selenide mineralisation; O-free halides are known only in volcanic fumaroles and oxygen compounds form in the oxidation zone of Tl-bearing ores or in fumaroles.

In this paper we describe a new hydrous chloride of potassium and trivalent thallium found in fumarolic deposits at the Tolbachik volcano, Kamchatka, Russia. Its name kalithallite (Russian Cyrillic: калиталлит) reflects the important crystal chemical feature: this is a *kalium–thallium* ordered compound (*kalium*, the Latin name of potassium is used for the name construction). Both the mineral and its name (symbol Kth) have been approved by the IMA Commission on New Minerals, Nomenclature and Classification (IMA2017–044, Pekov *et al.*, 2017). Kalithallite became the third mineral with species-defining trivalent thallium, after avicennite  $Tl_2O_3$  (Karpova *et al.*, 1958) and chrysothallite  $K_6Cu_6Tl^{3+}Cl_{17}(OH)_4 \cdot H_2O$  (Pekov *et al.*, 2015c). Recently a fourth mineral with  $Tl^{3+}$  was discovered, amgaite  $Tl_2^{3+}Te^{6+}O_6$  (Kasatkin *et al.*, 2022). All these four minerals are extremely rare in Nature due to the particular and unusual

\*Author for correspondence: Igor V. Pekov, Email: [igorpekov@mail.ru](mailto:igorpekov@mail.ru)

†Deceased 20 March 2021

Cite this article: Pekov I.V., Krzhizhanovskaya M.G., Yapaskurt V.O., Belakovskiy D.I., Sidorov E.G. and Zhegunov P.S. (2023) Kalithallite,  $K_3Tl^{3+}Cl_6 \cdot 2H_2O$ , a new mineral with trivalent thallium from the Tolbachik volcano, Kamchatka, Russia. *Mineralogical Magazine* 87, 186–193. <https://doi.org/10.1180/mgm.2022.124>

formation conditions, under very high oxidising potential necessary for the appearance of  $Tl^{3+}$ ; all other known minerals with species-defining Tl contain this element in univalent form.

Fumarolic thallium mineralisation is unique, endemic: Tl minerals belonging to this genetic type are unknown elsewhere. Three  $Tl^+$  minerals were first described in sublimes of fumaroles at the La Fossa crater, Vulcano island, Aeolian archipelago, Italy, namely lafossaite  $Tl(Cl,Br)$  (Roberts *et al.*, 2006), hephaistosite  $TlPb_2Cl_5$  (Campostrini *et al.*, 2008), and steropesite  $Tl_3BiCl_6$  (Demartin *et al.*, 2009). At the Tolbachik volcano, besides chrysothallite and kalithallite containing  $Tl^{3+}$ , three minerals with univalent thallium were discovered: markhininite  $TlBi(SO_4)_2$ , karpovite  $Tl_2VO(SO_4)_2(H_2O)$ , and evdokimovite  $Tl_4(VO)_3(SO_4)_5(H_2O)_5$  (Siidra *et al.*, 2014a, 2014b, 2014c). Nataliyamalikitite TlI was found in an active fumarole at the Avacha (Avachinskiy) volcano, Kamchatka, Russia (Okrugin *et al.*, 2017).

The type specimen of kalithallite is deposited in the systematic collection of the Fersman Mineralogical Museum of the Russian Academy of Sciences, Moscow with the catalogue number 96192.

### Occurrence

Kalithallite is a very rare mineral. It was found in only three specimens collected by us in July 2013 from an active fumarole belonging to the Northern fumarole field located at the northern slope of the crater of the First scoria cone of the Northern Breakthrough of the Great Tolbachik Fissure Eruption, Tolbachik volcano, Kamchatka Peninsula, Far-Eastern Region, Russia. This scoria cone, a monogenetic volcano ~300 m high and ~0.1 km<sup>3</sup> in volume, was formed in 1975 (Fedotov and Markhinin, 1983) and still demonstrates strong fumarolic activity: many gas vents with temperatures up to 350°C occur around and inside its crater.

At the Northern fumarole field, the majority of strongly mineralised fumarole chambers occur at depths from 0.1 to 0.3 m below the day surface. In July 2013, our measurements, carried out using a chromel–alumel thermocouple, showed temperatures 180–250°C. The volcanic gas here is enriched by HCl and HF (Zelenski and Taran, 2012). The major minerals of sublimate incrustations, which partially or completely cover walls of the chambers, are sellaite, fluorite, halite and anhydrite. The elements

present, which also determine the geochemical specialisation of these oxidising-type fumaroles are Zn, Pb, Mn, Se and Tl. Cotunnite  $PbCl_2$ , sofiite  $Zn_3(Se^{4+}O_3)Cl_2$  and flinteite, including its Tl-bearing variety  $(K,Tl)_2ZnCl_4$ , are common here. Minor minerals are chubarovite  $KZn_2(BO_3)Cl_2$ , zincomenite  $ZnSeO_3$ , anglesite, hollandite  $Ba(Mn_6^{4+}Mn_2^{3+})O_{16}$ , challacolloite  $KPb_2Cl_5$ , saltonseaitite  $K_3NaMnCl_6$ , and sylvite, whereas olsacherite  $Pb_2(Se^{6+}O_4)(SO_4)$ , bixbyite-(Mn)  $Mn_2O_3$ , jakobssonite  $CaAlF_5$ , hieratite  $K_2SiF_6$ , hematite and baryte are very rare.

In the upper zone of the fumarole system (5–15 cm below the surface) our measurements showed the temperatures 30–100°C. Unlike the lower, hotter parts of the fumaroles in which only H-free minerals occur, in this upper zone we observe the associations of hydrous minerals. The major minerals present are gypsum, 'ralstonite' (hydrokenoralstonite)  $Na_{0.5}(Al,Mg)_2(F,OH)_6 \cdot H_2O$ , and opal. Subordinate minerals here are cryobostrixyite  $KZnCl_3 \cdot 2H_2O$ , vernadite (which forms pseudomorphs after saltonseaitite) and secondary halite and sylvite. Leonardsenite  $MgAlF_5 \cdot 2H_2O$  and kalithallite are found in minor amounts in small pockets in which the temperatures measured during the sampling were 70–100°C.

### General appearance, physical properties and optical data

Kalithallite overgrows the surface of basalt scoria, altered by fumarolic gas, in association with cryobostrixyite, halite, sylvite, opal and gypsum. The new mineral forms lamellar to tabular (flattened on [001]) crystals up to  $5 \times 30 \times 40 \mu m$ , sometimes with a stepped surface (Fig. 1). The major crystal form is the pinacoid {001}; faces of the tetragonal prisms {100} and {010} were observed, as well as non-indexed dipyrmidal faces. Kalithallite crystals are combined in open-work clusters or roundish aggregations up to 1 mm across (Figs 1b and 2).

Kalithallite is transparent, colourless in individuals, and white to pale cream-coloured or pale beige in aggregates. The streak is white. The lustre is vitreous. The mineral is brittle. Cleavage or parting were not observed, the fracture is uneven. Density calculated using the empirical formula is  $3.01 \text{ g cm}^{-3}$ .

Kalithallite is optically uniaxial (-),  $\epsilon = 1.656(3)$ , and  $\omega = 1.662(3)$  (589 nm). In transmitted light the mineral is colourless and non-pleochroic.

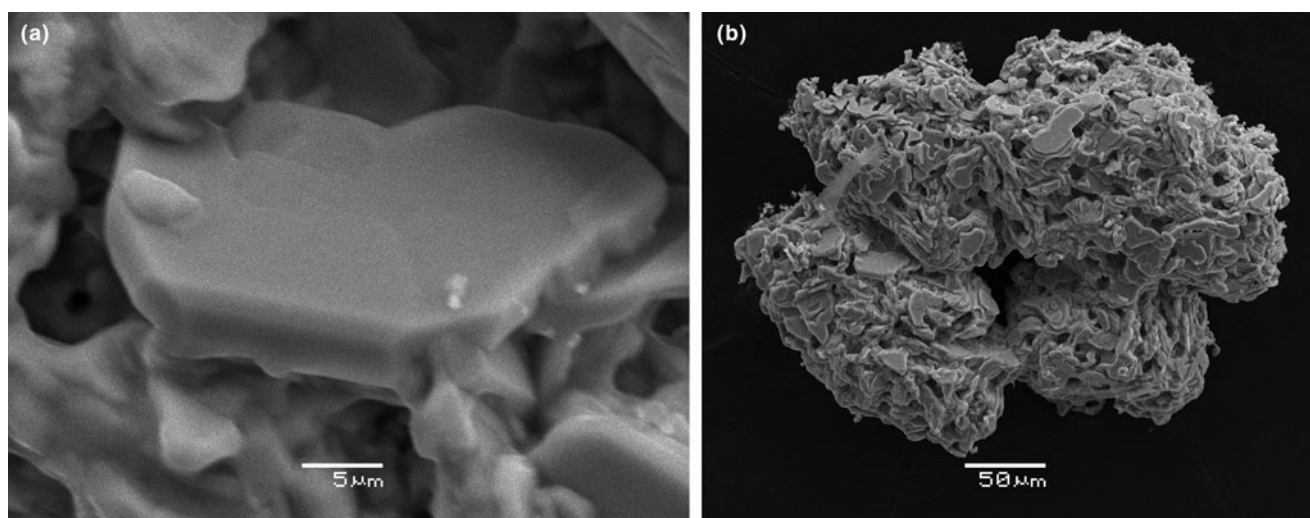
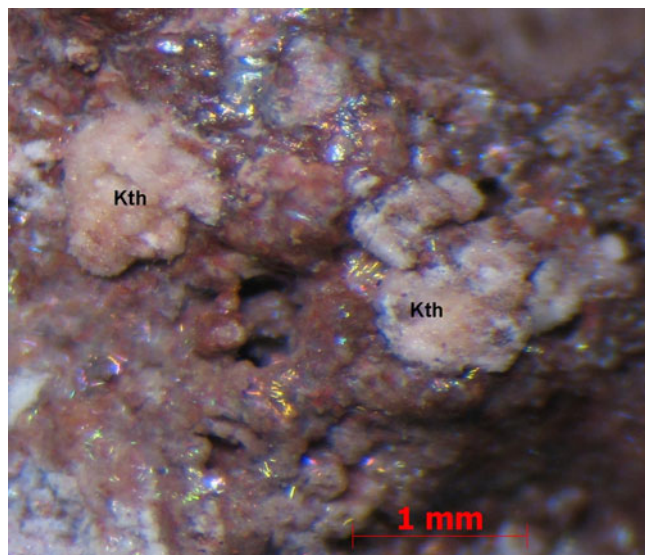


Fig. 1. Crystal (a) and open-work aggregate (b) of kalithallite. SEM images, secondary electron mode, holotype specimen #96192.



**Fig. 2.** Roundish aggregates of kalithallite (Kth) on basalt scoria altered by fumarolic gas and partially covered by thin colourless, aqua to transparent lustrous halite-sylvite crust. FOV width: 3.7 mm. Photo: I.V. Pekov & A.V. Kasatkin, holotype specimen #96192.

### Chemical data

Chemical data for kalithallite were obtained using a Jeol JSM-6480LV scanning electron microscope (SEM) equipped with an INCA-Wave 500 wavelength-dispersive spectrometer (Laboratory of Analytical Techniques of High Spatial Resolution, Dept. of Petrology, Moscow State University), with an acceleration voltage of 20 kV, a beam current of 10 nA and a 5  $\mu\text{m}$  beam diameter. The following standards were used: microcline (K), ZnSe (Zn),  $\text{TlAsS}_2$  (Tl) and NaCl (Cl). Contents of other elements with atomic numbers  $>4$ , except oxygen, are below detection limits.

The average (4 spot analyses) chemical composition of kalithallite (wt.%, ranges are in parentheses) is: K 17.72 (17.06–18.21), Zn 0.85 (0.76–0.98), Tl 38.76 (37.67–39.78), Cl 35.91 (35.09–36.47),  $\text{H}_2\text{O}_{\text{calc}}$  5.99, total 99.23.

$\text{H}_2\text{O}$  was not analysed because of the paucity of pure material. It was calculated by stoichiometry; the value is compatible with the crystal structure data (see below) and the correctness of the

calculation is indirectly confirmed by the analytical total close to 100 wt.%.

The empirical formula of kalithallite, calculated on the basis of  $\text{K}+\text{Zn}+\text{Tl}+\text{Cl}=10$  atoms per formula unit (apfu) with 2  $\text{H}_2\text{O}$  molecules pfu, is  $\text{K}_{2.72}\text{Zn}_{0.06}\text{Tl}_{1.14}\text{Cl}_{6.08}\cdot 2\text{H}_2\text{O}$ . It is noteworthy that, if all Tl could be considered as  $\text{Tl}^{3+}$ , then the total positive charge in this formula is +6.26 while the total negative charge is –6.08. This slight discrepancy could be caused by a general analytical error or due to the presence of a small part of the thallium in univalent form, which could substitute  $\text{K}^+$ . The formal recalculation of the empirical formula above according to the charge balance requirement gives the following formula:  $\text{K}_{2.72}\text{Zn}_{0.06}\text{Tl}_{0.09}^{+}\text{Tl}_{1.05}^{3+}\text{Cl}_{6.08}\cdot 2\text{H}_2\text{O}$ .

The idealised formula of kalithallite is  $\text{K}_3\text{Tl}^{3+}\text{Cl}_6\cdot 2\text{H}_2\text{O}$  which requires K 20.56, Tl 35.83, Cl 37.29,  $\text{H}_2\text{O}$  6.32, total 100 wt.%.

### X-ray crystallography and crystal structure determination

Attempts at single-crystal X-ray diffraction (XRD) studies of kalithallite were unsuccessful because of both the small size and imperfectness (probably due to a microblocky character) of crystals. The powder XRD data show that kalithallite is the natural counterpart of synthetic  $\text{K}_3\text{Tl}^{3+}\text{Cl}_6\cdot 2\text{H}_2\text{O}$  (tetragonal,  $I4/mmm$ ,  $a = 15.873$ ,  $c = 18.041$   $\text{\AA}$  and  $V = 4545$   $\text{\AA}^3$ ; Hoard and Goldstein, 1935). The crystal structure of the mineral was refined using the starting parameters of this synthetic compound.

Powder XRD studies of kalithallite were performed on a Rigaku R-Axis Rapid II single-crystal diffractometer equipped with a cylindrical image plate detector (radius 127.4 mm) using Debye-Scherrer geometry,  $\text{CoK}\alpha$  radiation (rotating anode with VariMAX microfocuss optics), 40 kV, 15 mA and an exposure time of 15 min. Angular resolution of the detector is  $0.045^\circ 2\theta$  (pixel size = 0.1 mm). The data were integrated using the software package *Osc2Tab* (Britvin et al., 2017). Powder X-ray diffraction data of kalithallite are given in Table 1.

The crystal structure of kalithallite was refined from the powder XRD data using the Rietveld method. The crystal structure of synthetic  $\text{K}_3\text{Tl}^{3+}\text{Cl}_6\cdot 2\text{H}_2\text{O}$  (Hoard and Goldstein, 1935) was used as a structure model. Data treatment and the Rietveld structure analysis were carried out using the program package *Topas 5.0* (Bruker, 2014). The powder sample studied contained ~6 wt.% of admixed sylvite. The peak profile was modelled using the Thompson-

**Table 1.** Powder X-ray diffraction data of kalithallite.

$l_{\text{obs}}$	$d_{\text{obs}}$ ( $\text{\AA}$ )	$l_{\text{calc}}^*$	$d_{\text{calc}}$ ( $\text{\AA}$ )	$hkl$
9	11.98	11	11.960	101
8	11.29	14	11.267	110
2	9.11	1	9.051	002
4	7.98	4	7.967	200
4	7.06	4	7.056	112
3	6.63	4	6.631	211
<b>100</b>	<b>5.98</b>	100	5.980	202
<b>36</b>	<b>5.64</b>	34	5.633	220
2	5.035	2	5.039	310
2	4.779	2	4.783	222
3	4.611	1	4.605	213
8	4.527	8	4.525	004
3	4.403	1	4.402	312
3	4.289	2	4.293	321
2	4.197	2	4.199	114
<b>20</b>	<b>3.984</b>	19	3.983	400

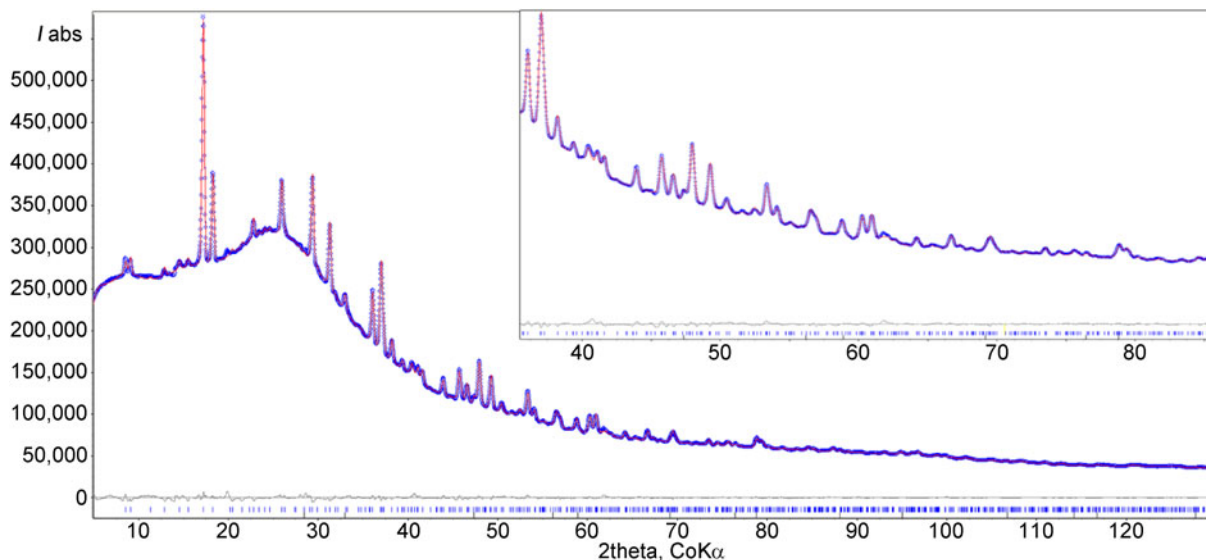
(Continued)

Table 1. (Continued.)

$l_{\text{obs}}$	$d_{\text{obs}}$ (Å)	$l_{\text{calc}}^*$	$d_{\text{calc}}$ (Å)	$hkl$
3	3.779	0.5	3.779	411
<b>30</b>	<b>3.528</b>	1, 32	3.530, 3.528	105, 224
4	3.469	1	3.469	332
<b>22</b>	<b>3.315</b>	25	3.315	422
3	3.257	1	3.254	413
2	3.014	1	3.017	006
2	2.991	1	2.990	404
<b>15</b>	<b>2.890</b>	22	2.890	334
<b>24</b>	<b>2.817</b>	11, 3, 23	2.821, 2.818, 2.817	206, 503, 440
6	2.732	10	2.733	530
1	2.690	0.5	2.689	442
3	2.655	4	2.656	600
1	2.618	1	2.616	532
4	2.587	1, 5	2.592, 2.588	611, 316
3	2.573	2	2.572	514
4	2.548	1, 4	2.553, 2.548	107, 602
4	2.519	6	2.519	620
1	2.466	0.5	2.465	541
4	2.391	2, 5	2.392, 2.391	505, 444
7	2.301	13, 0.5	2.302, 2.300	426, 543
5	2.262	10	2.263	008
3	2.226	1	2.218	118
<b>11</b>	<b>2.201</b>	22, 0.5	2.201, 2.187	624, 552
8	2.146	18	2.147	642
3	2.099	5	2.100	228
1	2.056	0.5, 0.5	2.057, 2.051	723, 545
2	2.023	3, 2	2.025, 2.017	536, 714
7	1.992	8, 6	1.993, 1.992	606, 800
3	1.967	6	1.967	408
1	1.934	0.5	1.936	219
5	1.888	8	1.890	822
3	1.877	6	1.878	660
4	1.822	7	1.823	804
5	1.782	8, 3	1.783, 1.781	646, 840
5	1.764	4, 9	1.765, 1.764	2.0.10, 448
2	1.742	3	1.743	538
2	1.734	3	1.734	664
1	1.722	0.5, 0.5, 1	1.723, 1.720, 1.719	2.2.10, 921, 736
2	1.684	5	1.683	628
1	1.657	0.5	1.658	844
3	1.628	0.5, 7	1.631, 1.627	3.3.10, 826
1	1.614	2	1.614	4.2.10
1	1.597	1	1.597	558
5	1.569	1, 0.5, 8, 2	1.575, 1.572, 1.569, 1.562	934, 3.0.11, 862, 10.2.0
2	1.538	0.5, 0.5, 0.5	1.540, 1.536, 1.535	10.2.2, 738, 639
2	1.521	1, 0.5	1.520, 1.516	916, 774
2	1.508	1	1.508	0.0.12
3	1.496	0.5, 5	1.496, 1.495	6.0.10, 808
2	1.479	0.5, 2	1.480, 1.477	10.3.3, 10.2.4
2	1.460	1, 2, 3	1.464, 1.460, 1.457	954, 10.4.2, 2.2.12
2	1.446	3	1.445	668
1	1.436	1	1.437	767
3	1.409	5, 2, 2	1.409, 1.408, 1.406	10.0.6, 880, 10.4.4
3	1.401	4, 0.5, 2, 0.5	1.400, 1.400, 1.400, 1.397	6.4.10, 3.3.12, 848, 11.3.0
1	1.389	1	1.389	918
1	1.367	1	1.366	10.6.0
2	1.345	2	1.345	884
2	1.330	2, 2, 1	1.330, 1.328, 1.328	4.4.12, 10.4.6, 12.0.0
2	1.323	2	1.321	8.2.10
2	1.295	3, 3	1.296, 1.294	12.2.2, 6.2.12
2	1.287	2	1.286	10.2.8
1	1.233	3, 0.5	1.233, 1.231	10.8.2, 9.3.10
1	1.214	2, 3	1.215, 1.214	4.2.14, 12.4.4
1	1.202	2, 2	1.203, 1.201	8.0.12, 12.2.6
1	1.197	4, 2	1.196, 1.196	10.0.10, 888
1	1.176	2, 0.5, 2	1.178, 1.177, 1.176	12.6.2, 3.0.15, 6.6.12

\*Only reflections with  $l_{\text{calc}} \geq 0.5$  are given; the strongest reflections are marked in bold type.





**Fig. 3.** Final Rietveld refinement plot of kalithallite with enlarged high-angle fragment. The red solid line corresponds to calculated data, the blue circles correspond to the observed pattern and the blue vertical bars mark all possible Bragg reflections. The difference between the observed and calculated patterns is shown as a curve over the bars.

Cox-Hastings pseudo-Voigt profile function. Coordinates and thermal parameters of H atoms were not refined. The correctness of both model and structure refinement is confirmed by very low values of final agreement factors ( $R_{\text{Bragg}} = 0.55\%$ ,  $R_p = 0.56\%$ , and  $R_{\text{wp}} = 0.75\%$  and  $R_{\text{exp}} = 0.28\%$ ). The observed and calculated powder XRD patterns (final Rietveld refinement plot) are shown in Fig. 3. Crystal data and Rietveld refinement details are given in Table 2, atom coordinates and displacement parameters in Table 3 and selected interatomic distances in Table 4. The crystallographic information files is supplied in Supplementary materials (see below)

## Discussion

### Crystal structure and comparative crystal chemistry

Kalithallite is a natural analogue of synthetic  $\text{K}_3\text{Tl}^{3+}\text{Cl}_6 \cdot 2\text{H}_2\text{O}$  (Hoard and Goldstein, 1935). Despite the absence of single-crystal XRD data on the mineral, this analogy is confirmed unambiguously by the stoichiometry and a very good agreement between the measured powder XRD pattern of kalithallite and the calculated data from Rietveld refinement with the use of the synthetic  $\text{K}_3\text{Tl}^{3+}\text{Cl}_6 \cdot 2\text{H}_2\text{O}$  crystal structure as the initial model (Table 1; Fig. 3).

The crystal structure of kalithallite (Fig. 4) contains octahedra  $\text{Tl}^{3+}\text{Cl}_6$  isolated from one another, with Tl–Cl distances varying

between 2.45 and 2.60 Å (Table 4). Such distances are typical for trivalent thallium. In the synthetic analogue of kalithallite the distances  $\text{Tl}^{3+}\text{–Cl}^-$  vary from 2.55 to 2.56 Å (Hoard and Goldstein, 1935) and in other well-studied synthetic chlorides are as follows:  $\text{KTl}^{3+}\text{Cl}_4$  2.42 (Glaser, 1980),  $\text{Tl}^+\text{Tl}^{3+}\text{Cl}_4$  2.42 (Thiele and Rink, 1975),  $\text{Tl}_3^+\text{Tl}^{3+}\text{Cl}_6$  2.51–2.73 (Boehme et al., 1980),  $\text{K}_2\text{Tl}^{3+}\text{Cl}_5 \cdot 2\text{H}_2\text{O}$  2.48–2.79 Å (Thiele and Grunwald, 1983). In contrast, the distances  $\text{Tl}^+\text{–Cl}^-$  in the same chlorides are as follows (for references see above):  $\text{Tl}^+\text{Tl}^{3+}\text{Cl}_4$  3.27–3.29 and  $\text{Tl}_3^+\text{Tl}^{3+}\text{Cl}_6$  3.03–3.83 Å. In  $\text{Tl}^+\text{Cl}$  the distances  $\text{Tl}^+\text{–Cl}^-$  vary between 3.15 and 3.72 Å (Ungelenk, 1962). Similar values were reported for natural  $\text{Tl}^+$  chlorides. In steropesite  $\text{Tl}_3\text{BiCl}_6$  the distances  $\text{Tl}^+\text{–Cl}^-$  in twelve  $\text{TlCl}_6$  polyhedra vary between 3.27 and 3.28 Å (Demartin et al., 2009). In hephaistosite  $\text{TlPb}_2\text{Cl}_5$ ,  $\text{Tl}^+$  is substituted by  $\text{K}^+$  for 14% and the mean  $(\text{Tl,K})^+\text{–Cl}^-$  distance is 3.325 Å (Camprostrini et al., 2008). Thus, the trivalent state of species-defining thallium in kalithallite is without doubt. One of three crystallographically independent thallium sites, Tl1

**Table 3.** Atomic positional coordinates and isotropic displacement parameters ( $B_{\text{iso}}$ , Å<sup>2</sup>) of kalithallite.

Site	Site				Site occupancy	$B_{\text{iso}}$
	multiplicity	x	y	z		
Tl1	2	0	0	0	$\text{Tl}_{0.66(1)}\text{Zn}_{0.34(1)}$	2.0(3)
Tl2	4	0	1/2	0	1	2.5(1)
Tl3	8	1/4	1/4	1/4	1	2.2(1)
Cl1	4	0	0	0.1353(11)	1	2.8(1)
Cl2	8	0.1579(8)	0	0	1	2.8(1)
Cl3	8	0	1/2	0.1391(6)	1	2.8(1)
Cl4	16	0.3847(3)	0.1153(3)	0	1	2.8(1)
Cl5	16	0.1798(2)	–0.1798(2)	0.3597(5)	1	2.8(1)
Cl6	16	0.1624(3)	–0.162(3)	0.1614(5)	1	2.8(1)
Cl7	16	0.3602(3)	0.8602(3)	1/4	1	2.8(1)
K1	8	0.2177(5)	0.2177(5)	0	0.90	4.3(4)
K2	16	0	0.2966(6)	0.1316(7)	0.93	4.2(4)
K3	16	0	0.2756(6)	0.3870(6)	1	4.5(4)
O1	4	0	0	0.409(2)	1	1.9(6)
O2	8	0.131(2)	0	1/2	1	1.9(6)
O3	16	0	0.154(1)	0.283(1)	1	1.9(6)

**Table 2.** Crystal data and Rietveld refinement details for kalithallite.

Formula	$\text{K}_{2.72}\text{Zn}_{0.05}\text{Tl}_{0.95}\text{Cl}_6 \cdot 2\text{H}_2\text{O}^*$
Crystal system, space group, Z	Tetragonal, $I4/mmm$ , 14
Unit cell dimensions (Å)	$a = 15.9333(6)$ $c = 18.1008(8)$
Unit cell volume (Å <sup>3</sup> )	4595.2(4)
Diffractometer, wavelength	Rigaku R-AXIS Rapid II, 1.79021 Å
Temperature (K)	273
2 theta range (°)	5–130
$R_{\text{exp}} / R_{\text{wp}} / R_p$ (%)	0.28 / 0.75 / 0.56
$R_{\text{Bragg}}$ (%)	0.55

\*Slight charge disbalance in this formula is probably caused by the not very high quality of the experimental data.

**Table 4.** Selected bond lengths (Å) and bond valence sums (BVS\*, in valence units) in the structure of kalithallite.

Bond	Length (Å)	BVS (vu)	Bond	Length (Å)	BVS (vu)
Tl1–Cl1	2.449(19) ×2	0.54	K1–Cl4	3.119(8) ×2	0.22
Tl1–Cl2	2.516(13) ×4	0.45	K1–Cl6	3.180(10) ×2	0.19
Average/Total	<2.494>	2.88	K1–Cl5	3.427(10) ×2	0.1
			K1–Cl2	3.601(10) ×2	0.06
			Average/Total	<3.332>	1.02
Tl2–Cl3	2.518(12) ×2	0.57	K2–Cl2	3.249(10)	0.15
Tl2–Cl4	2.598(7) ×4	0.47	K2–Cl3	3.244(17)	0.15
Average/Total	<2.571>	3.06	K2–Cl4	3.320(11) ×2	0.12
			K2–Cl6	3.400(16) ×2	0.1
			K2–Cl7	3.253(12) ×2	0.15
			K2–O3	3.537(12)	0.01
			Average/Total	<3.331>	0.97
Tl3–Cl5	2.537(4) ×2	0.56	K3–O2	2.727(20)	0.13
Tl3–Cl6	2.544(8) ×2	0.55	K3–O3	3.080(20)	0.05
Tl3–Cl7	2.483(7) ×2	0.64	K3–Cl3	3.610(16)	0.05
Average/Total	<2.521>	3.50	K3–Cl4	3.253(12) ×2	0.14
			K3–Cl5	3.284(13) ×2	0.13
			K3–Cl7	3.596(12) ×2	0.05
			Average/Total	<3.298>	0.87

\*Bond-valence parameters were taken from Brese and O'Keeffe (1991).

probably contains admixed Zn (Table 3), which is in agreement with electron microprobe data. The position Tl1 seems to be the most suitable for the location of admixed Zn because it has the smallest size of the three Tl positions. The bond valence sum calculations for all Tl sites (Table 4) confirm this.

Potassium cations in kalithallite are in the centre of three types of polyhedra:  $\text{KCl}_8$ ,  $\text{KCl}_8(\text{H}_2\text{O})$ , and  $\text{KCl}_7(\text{H}_2\text{O})_2$  with average cation–anion distances 3.332, 3.331 and 3.298 Å, respectively

(Table 4). The potassium sites K1 and K2 demonstrate incomplete occupancy (Table 3) that is in agreement with some deficiency of potassium found from electron microprobe data resulting in the empirical formula  $\text{K}_{2.72}\text{Zn}_{0.06}\text{Tl}_{1.14}\text{Cl}_{6.08}\cdot 2\text{H}_2\text{O}$ . In the potassium arrangement, the mineral differs slightly from synthetic  $\text{K}_3\text{Tl}^{3+}\text{Cl}_6\cdot 2\text{H}_2\text{O}$ , which contains four independent  $\text{K}^+$  sites (Hoard and Goldstein, 1935): in kalithallite, one of them (2b: 0,0,0.5) is empty (or almost empty, it seems impossible to conclude exactly from

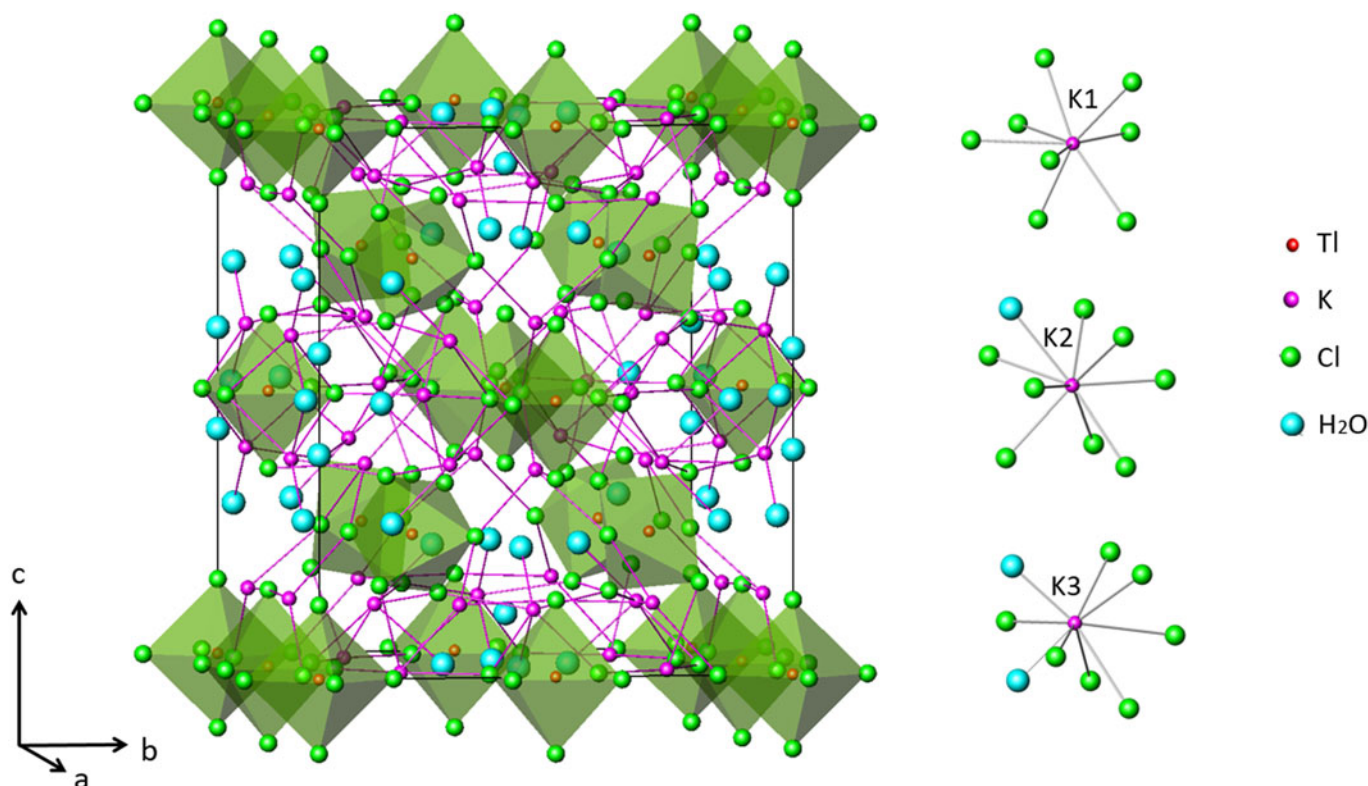


**Fig. 4.** The crystal structure of kalithallite and the potassium coordination polyhedra;  $\text{Tl}^{3+}\text{Cl}_6$  octahedra are shown as semi-transparent. The unit cell is outlined.

only Rietveld refinement without single-crystal data) and thus is not included in Table 3.

Kalithallite and its synthetic end-member analogue  $K_3Tl^{3+}Cl_6 \cdot 2H_2O$  are very close in terms of structure to two hydrous chlorides of K and  $In^{3+}$ , namely  $K_3InCl_6 \cdot H_2O$  (Wignacourt et al., 1980) and  $K_3InCl_6 \cdot 1.57H_2O$  (Knop et al., 1987). Both these K–In compounds adopt the tetragonal space group  $I4mm$  and are comparable in unit-cell dimensions to  $K_3Tl^{3+}Cl_6 \cdot 2H_2O$ . A smaller ionic radius for  $In^{3+}$  in comparison with  $Tl^{3+}$  could be the cause of lower  $H_2O$  content in these K–In chlorides in comparison to isotopic K–Tl chloride.

The trivalent state of thallium causes the K–Tl ordering in kalithallite which is the second mineral, after chrysothallite (Pekov et al., 2015c), with species-defining K and  $Tl^{3+}$  in different positions in the structure.

### Some notes on genesis

Kalithallite was found in the upper part of an active fumarole where the temperatures measured during the collecting were 70–100°C. The presence of  $H_2O$  in the mineral indicates that it was formed not as a result of direct deposition from volcanic gas at high temperatures (above 180–200°C), but as a secondary phase, a product of the reaction between sublimates, atmospheric water or water vapour and volcanic gas at relatively low temperatures, not higher than 100–150°C (for details see: Pekov et al., 2020). In other words, kalithallite was formed as a result of the combination of endogene (fumarolic) and supergene processes.

The Tl-enriched variety of flinteite,  $(K,Tl)_2ZnCl_4$ , which contains up to 27.7 wt.% Tl (Pekov et al., 2015a), is the most probable source of thallium for kalithallite. Flinteite, a common high-temperature mineral and the major concentrator of thallium in the primary assemblage of the fumaroles discussed here, is easily soluble in water and unstable in humid air. The close association of kalithallite with crybostryxite  $KZnCl_3 \cdot 2H_2O$ , the most typical product of low-temperature alteration of flinteite (Pekov et al., 2015b), confirms that the Tl-bearing variety of the latter could be a ‘precursor’ for the formation of kalithallite.

The presence of  $Tl^{3+}$  in kalithallite clearly demonstrates strongly oxidising conditions of mineral formation. As a result of the reaction with heated atmospheric oxygen,  $Tl^+$  mobilised from flinteite could be oxidised to  $Tl^{3+}$ . The evolution series ‘Tl-bearing flinteite  $(K,Tl)_2ZnCl_4 \rightarrow$  kalithallite  $K_3Tl^{3+}Cl_6 \cdot 2H_2O$  + crybostryxite  $KZnCl_3 \cdot 2H_2O$ ’ is a positive indicator of the significant increase of oxidising potential in this mineral-forming system from a high-temperature stage (>180–200°C), when minerals (including flinteite) deposit directly from hot fumarolic gas, to a relatively low-temperature stage (70–150°C) in which the complex interactions between volcanic gas, atmospheric agents and earlier formed sublimate minerals occur. It is noteworthy that chrysothallite  $K_6Cu_6Tl^{3+}Cl_{17}(OH)_4 \cdot H_2O$  crystallised at the same relatively low-temperature stage in Cu-enriched oxidising-type fumaroles on the Second scoria cone adjacent to the First scoria cone of the Northern Breakthrough of the Great Tolbachik Fissure Eruption (Pekov et al., 2015c).

**Acknowledgements.** We thank anonymous referees, Associate Editor Owen Missen and Principal Editor Stuart Mills for their valuable comments. The mineralogical study of kalithallite by IVP was supported by the Russian Science Foundation, grant no. 19-17-00050. The technical support by the SPbSU X-Ray Diffraction Resource is acknowledged.

**Supplementary material.** To view supplementary material for this article, please visit <https://doi.org/10.1180/mgm.2022.124>

**Competing interests.** The authors declare none.

### References

- Boehme R., Rath J., Grunwald B. and Thiele G. (1980) Über zwei Modifikationen von  $Tl_2Cl_3$  – valenzgemischten Thallium(I)-hexahalogenothallaten(III)  $Tl_3(TlCl_6)$ . *Zeitschrift für Naturforschung, Teil B. Anorganische Chemie, Organische Chemie*, **35**, 1366–1372.
- Brese N.E. and O’Keeffe M. (1991) Bond-valence parameters for solids. *Acta Crystallographica*, **B47**, 192–197.
- Britvin S.N., Dolivo-Dobrovolsky D.V. and Krzhizhanovskaya M.G. (2017) Software for processing the X-ray powder diffraction data obtained from the curved image plate detector of Rigaku RAXIS Rapid II diffractometer. *Zapiski Rossiiskogo Mineralogicheskogo Obshchestva*, **146**, 104–107 [in Russian].
- Bruker AXS (2014) *Topas 5.0: General Profile and Structure Analysis Software for Powder Diffraction Data*. Karlsruhe, Germany.
- Campostrini I., Demartin F. and Gramaccioli C.M. (2008) Hephaistosite,  $TlPb_2Cl_5$ , a new mineral species from La Fossa crater, Vulcano, Aeolian Islands, Italy. *The Canadian Mineralogist*, **46**, 701–708.
- Demartin F., Gramaccioli C.M. and Campostrini I. (2009) Steropesite,  $Tl_3BiCl_6$ , a new thallium bismuth chloride from La Fossa crater, Vulcano, Aeolian islands, Italy. *The Canadian Mineralogist*, **47**, 373–380.
- Fedotov S.A. and Markhinin Y.K. (editors) (1983) *The Great Tolbachik Fissure Eruption*. Cambridge University Press, New York.
- Glaser J. (1980) Crystal and molecular structure of potassium tetrachlorothallate(III). *Acta Chemica Scandinavica*, **A34**, 75–76.
- Hoard J.L. and Goldstein L. (1935) The structure of potassium hexachlorothallate dihydrate. *Journal of Chemical Physics*, **3**, 645–649.
- Karpova Kh.N., Kon’kova E.A., Larkin E.D. and Savel’ev V.F. (1958) Avicennite, a new thallium mineral. *Doklady Akademii Nauk Uzbekskoi SSR*, **2**, 23–25 [in Russian].
- Kasatkin A.V., Anisimova G.S., Nestola F., Plášil J., Sejkora J., Škoda R., Sokolov E.P., Kondratieva L.A. and Kardashevskaya V.N. (2022) Amgaite, IMA 2021–104. CNMNC Newsletter No. 66, page 360. *Mineralogical Magazine*, **86**, 359–362.
- Knop O., Cameron T.S., Adhikesavalu D., Vincent B.R. and Jenkins J.A. (1987) Crystal chemistry of complex indium(III) and other M(III) halides, with a discussion of M–Cl bond lengths in complex M(III) chlorides and of the structures of and hydrogen bonding in  $(NH_4)_2[InCl_5(H_2O)]$ ,  $K_3InCl_6 \cdot nH_2O$ ,  $(MeNH_3)_4[InCl_6]Cl$ , and  $(Me_2NH)_4[InCl_6]Cl$ . *Canadian Journal of Chemistry*, **65**, 1527–1556.
- Okrugin V., Favero M., Liu A., Etschmann B., Plutachina E., Mills S., Tomkins A.G., Lukasheva M., Kozlov V., Moskaleva S., Chubarov M. and Brugger J. (2017) Smoking gun for thallium geochemistry in volcanic arcs: Nataliyamalikit, TII, a new thallium mineral from an active fumarole at Avacha Volcano, Kamchatka Peninsula, Russia. *American Mineralogist*, **102**, 1736–1746.
- Pekov I.V., Zubkova N.V., Yapaskurt V.O., Britvin S.N., Vigasina M.F., Sidorov E.G. and Pushcharovsky D.Yu. (2015a) New zinc and potassium chlorides from fumaroles of the Tolbachik volcano, Kamchatka, Russia: mineral data and crystal chemistry. II. Flinteite,  $K_2ZnCl_4$ . *European Journal of Mineralogy*, **27**, 581–588.
- Pekov I.V., Zubkova N.V., Britvin S.N., Yapaskurt V.O., Chukanov N.V., Lykova I.S., Sidorov E.G. and Pushcharovsky D.Yu. (2015b) New zinc and potassium chlorides from fumaroles of the Tolbachik volcano, Kamchatka, Russia: mineral data and crystal chemistry. III. Crybostryxite,  $KZnCl_3 \cdot 2H_2O$ . *European Journal of Mineralogy*, **27**, 805–812.
- Pekov I.V., Zubkova N.V., Belakovskiy D.I., Yapaskurt V.O., Vigasina M.F., Lykova I.S., Sidorov E.G. and Pushcharovsky D.Yu. (2015c) Chrysothallite  $K_6Cu_6Tl^{3+}Cl_{17}(OH)_4 \cdot H_2O$ , a new mineral species from the Tolbachik volcano, Kamchatka, Russia. *Mineralogical Magazine*, **79**, 365–376.
- Pekov I.V., Krzhizhanovskaya M.G., Yapaskurt V.O., Belakovskiy D.I. and Sidorov E.G. (2017) Kalithallite, IMA 2017–044. CNMNC Newsletter No. 39, page 1280. *Mineralogical Magazine*, **81**, 1279–1286.

- Pekov I.V., Agakhanov A.A., Zubkova N.V., Koshlyakova N.N., Shchipalkina N.V., Sandalov F.D., Yapaskurt V.O., Turchkova A.G. and Sidorov E.G. (2020) Oxidizing-type fumaroles of the Tolbachik Volcano, a mineralogical and geochemical unique. *Russian Geology and Geophysics*, **61**, 675–688.
- Roberts A.C., Venance K.E., Seward T.M., Grice J.D. and Paar W.H. (2006) Lafossaite, a new mineral from the La Fossa Crater, Vulcano, Italy. *Mineralogical Record*, **37**, 165–168.
- Rudnick R.L. and Gao S. (2003) The Composition of the Continental Crust. In: *Treatise on Geochemistry*, 3, *The Crust* (Holland, H.D. and Turekian, K.K., editors). Elsevier-Pergamon, Oxford, UK.
- Siidra O.I., Vergasova L.P., Krivovichev S.V., Kretser Y.L., Zaitsev A.N. and Filatov S.K. (2014a) Unique thallium mineralization in the fumaroles of Tolbachik volcano, Kamchatka peninsula, Russia. I. Markhininite,  $Tl^+Bi(SO_4)_2$ . *Mineralogical Magazine*, **78**, 1687–1698.
- Siidra O.I., Vergasova L.P., Kretser Y.L., Polekhovskiy Y.S., Filatov S.K. and Krivovichev S.V. (2014b) Unique thallium mineralization in the fumaroles of Tolbachik volcano, Kamchatka peninsula, Russia. II. Karpovite,  $Tl_2VO(SO_4)_2(H_2O)$ . *Mineralogical Magazine*, **78**, 1699–1709.
- Siidra O.I., Vergasova L.P., Kretser Y.L., Polekhovskiy Y.S., Filatov S.K. and Krivovichev S.V. (2014c) Unique thallium mineralization in the fumaroles of Tolbachik volcano, Kamchatka peninsula, Russia. III. Evdokimovite,  $Tl_4(VO)_3(SO_4)_5(H_2O)_5$ . *Mineralogical Magazine*, **78**, 1711–1724.
- Thiele G. and Grunwald B. (1983) Über die Pentachlorothallate(III)  $K_2TlCl_5 \cdot 2H_2O$  und  $M_2TlCl_5 \cdot H_2O$  (M = Rb,  $NH_4$ ). *Zeitschrift für Anorganische und Allgemeine Chemie*, **498**, 105–114.
- Thiele G. and Rink W. (1975) Die Kristallstruktur von Thalliumdichlorid,  $TlCl_2$ . *Zeitschrift für Anorganische und Allgemeine Chemie*, **414**, 231–235.
- Ungelenk J. (1962) Zur Polymorphie der Thalliumhalogenide in Aufdampfschichten. *Naturwissenschaften*, **49**, 252–253.
- Wignacourt J.P., Novogorocki G., Mairesse G. and Barbier P. (1980) Evidence for ionic isomerism in complex salts. X-ray evidence in  $K_3InCl_6 \cdot H_2O$ . *Reviews in Inorganic Chemistry*, **2**, 207–217.
- Zelenski M. and Taran Y. (2012) Volcanic emissions of molecular chlorine. *Geochimica et Cosmochimica Acta*, **87**, 210–226.
- Zemann J. (1993) Thallium in Mineralogie und Geochemie. *Mitteilungen der Österreichischen Mineralogischen Gesellschaft*, **138**, 75–91.